

Acoustic plasmonics of Au grating/Bi_2Se_3 thin film/sapphire hybrid structures

Weiwu Li(李伟武), Konstantin Riegel, Chuanpu Liu(刘传普), Alexey Taskin, Yoichi Ando, Zhimin Liao(廖志敏), Martin Dressel, Yuan Yan(严缘)

Citation: Chin. Phys. B . 2020, 29(6): 067801 . **doi:** 10.1088/1674-1056/ab8a3c
Journal homepage: http://cpb.iphy.ac.cn; http://iopscience.iop.org/cpb

What follows is a list of articles you may be interested in

Effects of thickness & shape on localized surface plasmon resonance of sexfoil nanoparticles

Yan Chen(陈艳), Xianchao Liu(刘贤超), Weidong Chen(陈卫东), Zhengwei Xie(谢征微), Yuerong Huang(黄跃容), Ling Li(李玲)

Chin. Phys. B . 2017, 26(1): 017807 . **doi:** 10.1088/1674-1056/26/1/017807

Multifunctional disk device for optical switch and temperature sensor

Bian Zhen-Yu, Liang Rui-Sheng, Zhang Yu-Jing, Yi Li-Xuan, Lai Gen, Zhao Rui-Tong

Chin. Phys. B . 2015, 24(10): 107801 . **doi:** 10.1088/1674-1056/24/10/107801

Spatially nonlocal effects on optical absorption properties incoupled quantum wells with an applied electric field

Wang Chao-Yang, Wang Guang-Hui

Chin. Phys. B . 2014, 23(12): 127103 . **doi:** 10.1088/1674-1056/23/12/127103

Numerical investigation of the enhanced unidirectional surface plasmon polaritons generator

Zhang Zhi-Dong, Wang Hong-Yan, Zhang Zhong-Yue, Wang Hui

Chin. Phys. B . 2014, 23(1): 017801 . **doi:** 10.1088/1674-1056/23/1/017801

A compact frequency selective stop-band splitter by using Fabry–Perot nanocavity in a T-shape waveguide

M Afshari Bavil, Sun Xiu-Dong

Chin. Phys. B . 2013, 22(4): 047808 . **doi:** 10.1088/1674-1056/22/4/047808

SPECIAL TOPIC — Topological 2D materials

Acoustic plasmonics of Au grating/Bi_2Se_3 thin film/sapphire hybrid structures*

Weiwu Li(李伟武)[1], Konstantin Riegel[1], Chuanpu Liu(刘传普)[2], Alexey Taskin[3], Yoichi Ando[3], Zhimin Liao(廖志敏)[2], Martin Dressel[1], and Yuan Yan(严缘)[1,4,5,†]

[1] *Physikalisches Institut, Universität Stuttgart, Pfaffenwaldring* 57, 70550 *Stuttgart, Germany*
[2] *State Key Laboratory for Mesoscopic Physics, School of Physics, Peking University, Beijing* 100871, *China*
[3] *Physics Institute II, University of Cologne*, 50937 *Köln, Germany*
[4] *Physikalisches Institut der Universität Würzburg*, 97074 *Würzburg, Germany*
[5] *Institute for Topological Insulators*, 97074 *Würzburg, Germany*

(Received 11 February 2020; revised manuscript received 23 March 2020; accepted manuscript online 16 April 2020)

The surface plasmon polaritons of the topological insulator Bi_2Se_3 can be excited by using etched grating or grave structures to compensate the wave vector mismatch of the incident photon and plasmon. Here, we demonstrate novel gold grating/Bi_2Se_3 thin film/sapphire hybrid structures, which allow the excitation of surface plasmon polaritons propagating through nondestructive Bi_2Se_3 thin film with the help of gold diffractive gratings. Utilizing periodic Au surface structures, the momentum can be matched and the normal-incidence infrared reflectance spectra exhibit pronounced dips. When the width of the gold grating W (with a periodicity $2W$) increases from 400 nm to 1500 nm, the resonant frequencies are tuned from about 7000 cm^{-1} to 2500 cm^{-1}. In contrast to the expected $\sqrt{q}$ dispersion for both massive and massless fermions, where $q \sim \pi/W$ is the wave vector, we observe a sound-like linear dispersion even at room temperature. This surface plasmon polaritons with linear dispersion are attributed to the unique noninvasive fabrication method and high mobility of topological surface electrons. This novel structure provides a promising application of Dirac plasmonics.

Keywords: surface plasmon polaritons, topological insulator, infrared optoelectronics, nanophotonics

PACS: 78.68.+m, 71.35.Cc, 71.36.+c, 78.66.–w **DOI:** 10.1088/1674-1056/ab8a3c

1. Introduction

The low-dissipation massless Dirac electrons,[1–10] which are protected against scattering off nonmagnetic impurities, enable topological insulators (TIs) as an intriguing platform for plasmonics and photodetectors; for that reason they attract enormous attention from both experimental and theoretical physicists.[11–15] Plasmons are collective charge-density oscillations in solids under the influence of an electromagnetic field. With light shining on the topological surface state, the surface plasmon polaritons (SPPs) can be achieved using Kretschmann or Otto configuration, or etched grating[16] or grave structures[17] to compensate the wave vector mismatch of the photon and SPPs.

It was shown that SPPs can be created in TI in a wide energy range, from terahertz[16,18] to the ultraviolet,[17] promising far-reaching impact. In addition, due to the lower intrinsic bulk-carrier concentration in TIs, the resonant frequencies of SPPs can be electrically adjusted over a large range employing a gate voltage similar to a field effect transistor (FET).[19–21] However, so far, the existing experimental results for SPP in TIs are rather controversial because of the bulk conduction introduced by defects and impurities during the lithography process.[13] None of them provides unambiguous evidence for the SPP of pure Dirac electrons, although interesting physical phenomenon could potentially be discovered by taking a deeper look at them.

In this work, we introduce a novel path of drastically reducing the impurities and defects by using different processes to create a new structure, theoretically capable of exciting TI surface states. When compared to preceding plasmonics behavior in Bi_2Se_3 films with thickness about 60 nm or more, the novel thin film samples used here assure less bulk-carrier contributions, as they provide a higher surface to bulk ratio. An additional enhancement of the propagation length can be achieved when working with these thin films. The present study investigates the width-dependent plasmonic behavior of gold grating/Bi_2Se_3 thin film/sapphire hybrid structures in the infrared (IR) range using a Fourier-transform spectrometer: the acoustic plasmonics are observed at different temperatures.

2. Methods

High quality 11-nm-thick Bi_2Se_3 thin film was grown via molecular beam epitaxy on 0.47-mm-thick $Al_2O_3(111)$ by two-step deposition, with its thickness estimated from the Kiessig fringes.[22] To excite SPPs in Bi_2Se_3 thin films with

*Project supported by Carl-Zeiss-Stiftung.
†Corresponding author. E-mail: yuan.yan@physik.uni-wuerzburg.de
© 2020 Chinese Physical Society and IOP Publishing Ltd

a free-space infrared beam, rather than etching the thin TI film into stripes, we fabricated gold diffractive gratings with a thickness of 100 nm on top of the thin film in order to compensate for wave vector mismatches. By avoiding etching and lithography processes directly on the Bi_2Se_3 thin film, which are prone to creating defects and degradation of the quality of TI surface states, fewer impurities and less bulk contributions are expected compared to its predecessors.

The width of the Au gratings is $W = 400$ nm, 600 nm, 800 nm, 1000 nm, 1200 nm, and 1500 nm, with period $2W$, as shown in Figs. 1(a) and 1(b), to obtain a series of discrete wavevector values of $q \sim \pi/W$. This hybrid structure with an 11 nm-thick Bi_2Se_3 thin film is here after referred to as "TI-sample". For comparison, the same gold diffractive gratings are fabricated directly on bare sapphire substrate with the exact processes, which is named as "Ref-sample" for the rest of this work.

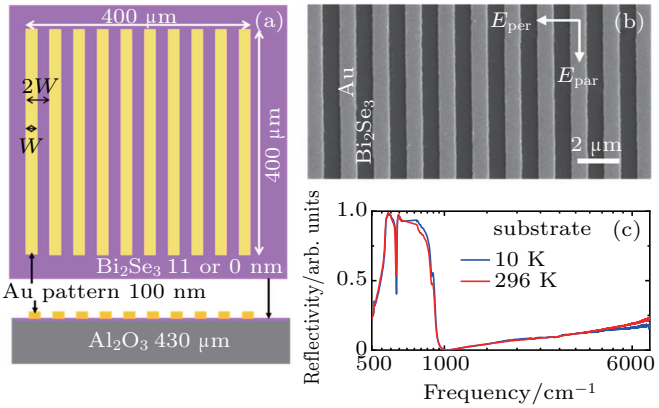


Fig. 1. (a) Schematic structure of the Ref-sample (without Bi_2Se_3 thin film) and TI-sample (with 11-nm-thick Bi_2Se_3 thin film) with dimensions of 400 μm by 400 μm. The width of the Au gratings is $W = 400$ nm, 600 nm, 800 nm, 1000 nm, 1200 nm, and 1500 nm, with period $2W$. (b) The scanning electron microscopy (SEM) image of the grating structures with notation of incident light parallel or perpendicular to the ribbon direction. (c) The reflectivity of bare sapphire substrate at $T = 10$ K and 296 K in the spectral range from 500 cm^{-1} to 7100 cm^{-1}.

The reflectivity of our samples was recorded in the IR-range (500 cm^{-1}–8000 cm^{-1}) with normal-incident light polarized both parallel and perpendicular to the ribbon extension. The measurements were performed with the Bruker Vertex80v Fourier transform spectrometer, equipped with a Hyperion 2000 infrared microscope and a CryoVac helium cryostat covering the temperature range from 10 K to 296 K. SPPs can be excited only when the incident light is polarized perpendicular to the grating lines; they can be seen as a dip in the reflectivity spectrum.

3. Results and discussion

The reflectivity of the bare sapphire substrate at $T = 10$ K and 296 K in the range of 500 cm^{-1} to 7100 cm^{-1} is shown Fig. 1(c). As expected, no difference in reflection is observed between parallel and perpendicular polarized beams. Sapphire has a relatively low reflectivity as typical for insulators. The dip at about 633 cm^{-1} is due to the excitation of an intrinsic phonon mode of Al_2O_3.[23]

In Fig. 2, the reflectivity of the Ref-sample (panels (a) and (b)) and TI-samples (panels (c) and (d)) are shown as obtained at different temperatures under parallel and perpendicular polarized incident light. For the parallel polarization (Figs. 2(b) and 2(d)), the spectra of both samples display a high reflectivity – as characteristic for metals – with the substrate phonon mode at about 633 cm^{-1} barely visible; providing evidence that the incident light interacts mainly with the grating and TI-film. In the mid-infrared range, the reflectivity of both samples decreases to lower values, with broad dips that vary in accordance to the ribbon-width. It is clear that these dips are not caused by surface plasmon excitations, because no resonance features are expected with the light polarizing along the grating lines. These dips might be induced by diffraction (for short wavelengths) and/or scattering (for long wavelengths) of the incident light on our structures. Consequently, the incident light is led astray and not detected as reflected light, resulting in a dip, which is beyond the interest of this work. For the perpendicular polarization, the Ref-sample (Fig. 2(a)) and the TI-sample (Fig. 2(c)) show very similar behaviors below 1000 cm^{-1}. Above 1000 cm^{-1}, the grating width-dependent peaks with steep rising front and falling front observed in both Ref-sample and TI-sample are attributed to the first-order Rayleigh anomalies.[24] In addition to the Rayleigh anomalies, only the TI-sample exhibits a pronounced dip in the reflectivity spectrum, which clearly shifts for different grating widths and is the focus of this work. In accord with previous reports,[16] no pronounced temperature dependency of the reflectivity is observed in the TI-sample, which is taken as evidence for the robustness of the topological surface states.

Let us first focus on the low-frequency region. In Figs. 3(a) and 3(b), the reflectivity of both samples with various grating widths is replotted in the far-infrared spectral range from 540 cm^{-1} to 650 cm^{-1} on a magnified scale. On the left side of the intrinsic phonon mode of sapphire,[23] resonant modes can be identified with central frequencies that red-shift as the grating width increases. Compared to the Ref-sample with the same ribbon width, broadening and hardening of these resonant modes in the TI-sample are observed, as displayed in Fig. 3(c). Since these resonant modes exist even without the presence of Bi_2Se_3 thin film (but not in bare substrate), they are related to the gold gratings rather than the SPP of the Bi_2Se_3 thin film. Meanwhile, based on the phase-matching condition for SPP excitation:[25] $k \sin\theta + mq = k_{spp}$, where k is the wave vector of the incident radiation, θ is the incident angle, m is the diffraction order, and k_{spp} is the wave vector of SPP, the resonant frequencies of SPP from the gold grat-

ings are calculated to be in the near-infrared to visible range, which are beyond our measurement range. Consequently, we attribute these resonant modes to be the phonon-plasmon polariton, due to phonon of sapphire coupling with the gold SPP.[26,27] With 11-nm-thick Bi_2Se_3 thin film in between the gold gratings and substrate, the dielectric constant as well as the distance between the gold gratings and sapphire are modified, hence the resonant modes broaden and harden.

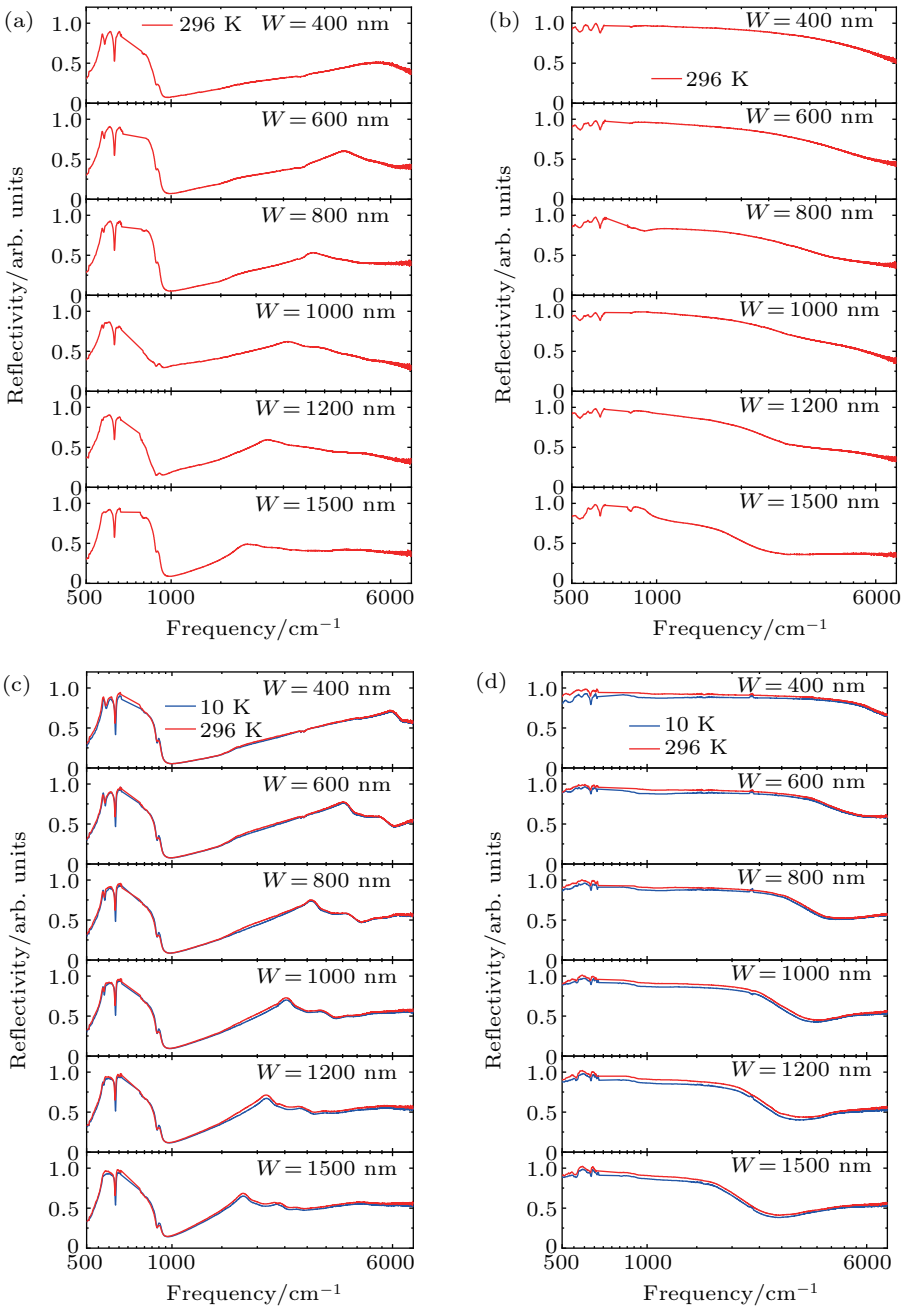


Fig. 2. Reflectivity spectra of the Ref-sample under perpendicularly (a) and parallelly (b) polarized incident light at different temperatures. The optical reflectivity of TI-sample under perpendicularly (c) and parallelly (d) polarized incident light at $T = 10$ K and 296 K.

In Figs. 4(a) and 4(4), the reflectivities of the Ref-sample and the TI-sample with different ribbon-widths are compared in the mid-infrared range. Unlike the resonant modes below 1000 cm^{-1} and the Rayleigh anomalies, in this spectral range the grating width-dependent plasmon-like dips are observed only in the TI-sample; hence we conclude that they originate from the 11-nm-thick Bi_2Se_3 thin film. The first idea is that these are the surface plasmon modes of the topological surface state observed by P. Di Pietro *et al.*[16] According to the calculation using random phase approximation theory, in the long-wavelength limit, the plasmon dispersion of the topological surface state is[16]

$$\nu_{\rm p} = \sqrt{\frac{\mu_{\rm F} e^2}{16\pi^2 \hbar \gamma_0 \gamma}} q \cdot (4\pi n_{\rm D})^{1/4}, \tag{1}$$

where $\mu_{\rm F}$ is the Fermi velocity, $\gamma = (\gamma_1 + \gamma_2)/2$ is the average electric permittivity of the vacuum (γ_1) and the substrate ($\gamma_2 \sim 10$), and $n_{\rm D}$ is the carrier concentration of the topological

surface state electrons. Assuming a carrier concentration and a Fermi velocity similar to those of P. Di Pietro *et al.*,[16] the surface plasmon excitations of our sample are estimated to fall in the range of 100–200 cm^{-1}. Even if the carrier concentration is higher by two orders of magnitude, the corresponding resonant frequencies (< 1000 cm^{-1}) are still much lower than our observation.

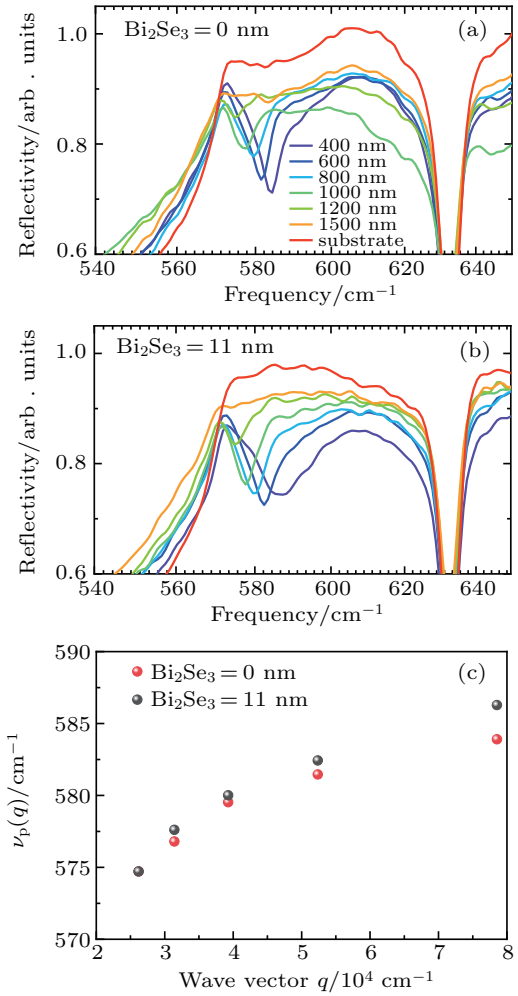


Fig. 3. The reflectivity of the Ref-sample (a) and the TI-sample (b) with various grating widths in the spectral range from 540 cm^{-1} to 650 cm^{-1}. (c) Comparison of resonant frequencies as a function of the grating width for Ref-sample and TI-sample.

In addition, we observe a linear increase of the bare plasmon frequencies with increasing wave vector $q = \pi/W$, as shown in Fig. 4(c). For both massive and massless fermions,[14,16] the dispersion relation should be $\nu_p \propto \sqrt{q}$. In other words, the mode we observed is not due to massive carriers either in the bulk states or the surface band bending. Instead, one might assume some lithography uncertainty of the grating width,[28] and hence try to fit our results with $q = \pi/(W - W_0)$, where W_0 is the difference between the design and real grating widths. We end up with W_0 about 12 nm, which is much smaller than the designed grating width (less than 3% error), and does not provide an explanation of the drastic deviation from the $\sqrt{q}$ dispersion behavior.

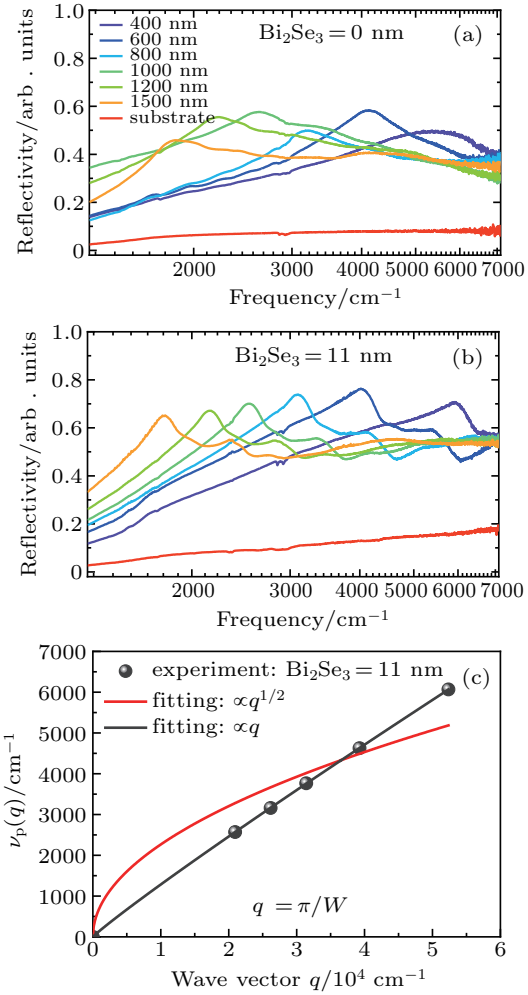


Fig. 4. The reflectivity of the Ref-sample (a) and the TI-sample (b) with various grating widths in the mid- and near-infrared ranges. (c) The bare plasmon frequencies are plotted versus wave vector $q = \pi/W$ and it has a linear dispersion rather than the predicted $\sqrt{q}$ dispersion behavior.

The linear dispersion relation between the plasmon frequencies and wave vector q resembles the dispersion behavior of acoustic plasmon modes, which could arise from different mechanisms. For TI thin films, plasmons are simultaneously excited on the top and bottom surfaces and hence can couple to each other. In this case, the existence of an optical plasmon mode (ν_+) and an acoustic plasmon mode (ν_-) was predicted with their corresponding dispersion relations[29–31]

$$\nu_+ = \sqrt{\frac{\mu_F e^2}{h\gamma_0(\gamma_T + \gamma_B + qd\gamma_{TI})}}q \cdot (2\pi n_D)^{1/4}, \tag{2}$$

$$\nu_- = \sqrt{\frac{2\gamma_0\gamma_{TI}h\mu_F + e^2\sqrt{2\pi n_D}d}{\sqrt{4\gamma_0^2\gamma_{TI}^2h^2\mu_F^2 + 2\gamma_0\gamma_{TI}e^2\sqrt{2\pi n_D}d}}}q. \tag{3}$$

These acoustic plasmon modes have been observed using electron energy loss spectroscopy.[32–35] However, as they do not carry an optical dipole matrix element; in other words, these modes do not couple to light and cannot be observed by standard optical experiments.[14] Another possibility would be the gapless acoustic-plasmon due to the screening effect excited by the gold grating layer on the SPP of Dirac electrons, as

in graphene.[19,36] Owing to the screened Coulomb interactions between electrons in graphene, a gapless acoustic plasmon with linear dispersion rather than an 'unscreened Dirac plasmon' is predicted. Considering the similarity between graphene and topological surface states, comparable screening effects due to the gold grating are expected. The dispersion relation calculated in graphene is[19,36] $\nu_{\rm ac} = c_{\rm s} q$, where $c_{\rm s} = \nu\sqrt{\frac{\Lambda(\alpha_{\rm ee} d k_{\rm F})}{\Lambda(\alpha_{\rm ee} d k_{\rm F})-1}}$, $\Lambda(x) = [1 + 1/(2 g_{\rm s} g_{\rm v} x)]^2 > 1$, $g_{\rm s}$ ($g_{\rm v}$) is the spin (valley) degeneracy factor, and ν is the Fermi velocity. Further calculations are expected to give the exact expression of $c_{\rm s}$ for the Bi_2Se_3 thin film.

4. Conclusion and perspectives

In our novel gold grating/Bi_2Se_3 thin film/sapphire hybrid structures, we have observed acoustic plasmon modes with a linear dispersion in the range from 1800 cm^{-1} to 4300 cm^{-1}; furthermore, we found one distinct mode at 590 cm^{-1} that results from coupling of substrate phonons and the intrinsic gold surface plasmons. The acoustic plasmon mode is reminiscent to the coupling between the plasmon of the top and bottom surfaces and the screening effect of the metal layer; at the present stage, we are not in the condition to make a final conclusion. We should note, however, that this is the first investigation on linear acoustic plasmon mode in topological insulator using Fourier-transform infrared spectrometer. Further experimental and theoretical investigations are strongly desired. Additional tuning of plasmon frequency using gate and/or TI thin film thickness is another way to elucidate the origin of the observed plasmon.

References

[1] Konig M, Wiedmann S, Brune C, Roth A, Buhmann H, Molenkamp L W, Qi X L and Zhang S C 2007 *Science* **318** 766
[2] Qi X L 2008 *Phys. Rev. B* **78** 195424
[3] Chen Y L, Analytis J G, Chu J H , Liu Z K, Mo S K , Qi X L, Zhang H J, Lu D H, Dai X, Fang Z, Zhang S C, Fisher I R, Hussain Z and Shen Z X 2009 *Science* **325** 178
[4] Hsieh D, Xia Y, Qian D, Wray L, Dil J, Meier F, Osterwalder J, Patthey L, Checkelsky J and Ong N 2009 *Nature* **460** 1101
[5] Hsieh D, Xia Y, Qian D, Wray L, Meier F, Dil J, Osterwalder J, Patthey L, Fedorov A and Lin H 2009 *Phys. Rev. Lett.* **103** 146401
[6] Zhang H, Liu C X, Qi X L, Dai X, Fang Z and Zhang S C 2009 *Nat. Phys.* **5** 438
[7] Hasan M Z and Kane C L 2010 *Rev. Mod. Phys.* **82** 3045
[8] Qi X L and Zhang S C 2010 *Phys. Today* **63** 33
[9] Yan Y, Liao Z M, Yu F, Wu H C, Jing G, Yang Z C, Zhao Q and Yu D 2012 *Nanotechnology* **23** 305704
[10] Yan, Y, Liao Z, Zhou Y, *et al.* 2013 *Sci. Rep.* **3** 1264
[11] Stauber T 2014 *J. Condens.: Matter Phys.* **26** 123201
[12] Deshko Y, Krusin-Elbaum L, Menon V, Khanikaev A and Trevino J 2016 *Opt. Express* **24** 7398
[13] Politano A, Viti L and Vitiello M S 2017 *APL Mater.* **5** 035504
[14] Ginley T, Wang Y, Wang Z and Law S 2018 *MRS Commun.* **8** 782
[15] Lai Y P , Lin I T , Wu K H and Liu J M 2014 *Nanomater. Nanotechnol.* **4** 13
[16] Di Pietro P, Ortolani M, Limaj O, Di Gaspare A, Giliberti V, Giorgianni F, Brahlek M, Bansal N, Koirala N and Oh S 2013 *Nat. Nanotech.* **8** 556
[17] Ou J Y, So J K, Adamo G, Sulaev A, Wang L and Zheludev N I 2014 *Nat. Commun.* **5** 5139
[18] In C, Sim S, Kim B, Bae H, Jung H, Jang W, Son M, Moon J, Salehi M and Seo S Y 2018 *Nano Lett.* **18** 734
[19] Grigorenko A, Polini M and Novoselov K 2012 *Nat. Photon.* **6** 749
[20] Ju L, Geng B, Horng J, Girit C, Martin M, Hao Z, Bechtel H A, Liang X, Zettl A and Shen Y R 2011 *Nat. Nanotech.* **6** 630
[21] Yan B, Fang J, Qin S, Liu Y, Chen L, Chen S, Li R and Han Z 2017 *Chin. Phys. B* **26** 097802
[22] Taskin A, Sasaki S, Segawa K and Ando Y 2012 *Adv. Mater.* **24** 5581
[23] Schubert M, Tiwald T E and Herzinger C M 2000 *Phys. Rev. B* **61** 8187
[24] Savoia S, Ricciardi A, Crescitelli A, Granata C, Esposito E, Galdi V and Cusano A 2013 *Opt. Express* **21** 23531
[25] Cao J, Kong Y and Gao S 2018 *Opt. Commun.* **406** 183
[26] Mikhailov S A 1998 *Phys. Rev. B* **58** 1517
[27] Brar V W, Jang M S, Sherrott M, Kim S, Lopez J J, Kim L B, Choi M and Atwater H 2014 *Nano Lett.* **14** 3876
[28] Yan H, Low T, Zhu W, Wu Y, Freitag M, Li X, Guinea F, Avouris P and Xia F 2013 *Nat. Photon.* **7** 394
[29] Stauber T, Gómez-Santos G and Brey L 2013 *Phys. Rev. B* **88** 205427
[30] Poyli M A, Hrtoň M, Nechaev I, Nikitin A Y, Echenique P M, Silkin V M, Aizpurua J and Esteban R 2018 *Phys. Rev. B* **97** 115420
[31] Raghu S, Chung S B, Qi X L and Zhang S C 2010 *Phys. Rev. Lett.* **104** 116401
[32] Jia X, Zhang S, Sankar R, Chou F C , Wang W, Kempa K, Plummer E, Zhang J, Zhu X and Guo J 2017 *Phys. Rev. Lett.* **119** 136805
[33] Politano A, Silkin V, Nechaev I, Vitiello M, Viti L, Aliev Z, Babanly M, Chiarello G, Echenique P and Chulkov E 2015 *Phys. Rev. Lett.* **115** 216802
[34] Kogar A, Vig S, Thaler A, Wong M, Xiao Y, Reig-i-Plessis D, Cho G, Valla T, Pan Z and Schneeloch J 2015 *Phys. Rev. Lett.* **115** 257402
[35] Glinka Y D, Babakiray S, Johnson T A, Holcomb M B and Lederman D 2016 *Nat. Commun.* **7** 13054
[36] Principi A, Asgari R and Polini M 2011 *Solid State Commun.* **151** 1627